Supplementary Information

TABLE S1. Water mediated hydrogen bonds[a] at the scFv 9004G-Cn2 interface

9004G location	9004G residue (atom)	Cn2 residue (atom)	Distance (Å/ Å)	B value (Å^2)
CDR H1	N31^H (OD1)	D7 (OD2)	3.3/2.8	33.1
	A33^H (N)	E15 (OE2)	3.0/2.9	16.8
CDR H2	R53^H (NH1)	K13 (O)	3.0/2.6	20.1
	R53^H (N)	E15 (O)	2.9/2.6	18.5
	S54^H (O)	Y24 (OH)	2.8/2.8	32.9
	D57^H (OD1)	Y24 (N)	3.3/3.3	22.6
framework H3	D59^H (OD1)	K18 (NZ)	2.9/3.3	42.7
	D59^H (OD2)	L17 (O)	3.1/2.6	23.1
CDR H3	V101^H (O)	A43 (O)	2.7/2.7	17.4
	G102^H (N)	E15 (OE1)	2.9/2.6	14.5
CDR L1	Y164^L (OH)	Y4 (OH)	2.8/2.7	26.1
CDR L3	R224^L (O)	A43 (N)	2.9/2.9	29.9
CDR L2	D182^L (OD1)	K13 (NZ)	2.7/2.8	42.3
	S226^L (OG)	L19 (N)	3.0/2.9	18.3
	R228^L (NH2)	C16 (O)	2.8/2.9	13.5

[a]Criteria based on donor-acceptor distances ≤ 3.5 Å.

TABLE S2. van der Waals contacts[a] between residues at the scFv 9004G-Cn2 interface

Cn2 residue[b]	9004G residue[b]
Y14 (2)	R53^H (2)
E15 (5)	A33^H (3), G99^H (1), V101^H (1)
L17 (8)	H35^H (1), W47^H (1), G50^H (3), I51^H (1), D57^H (1), D59^H (1)
K18 (7)	D57^H (4), I58^H (2), D59^H (1)
L19 (2)	Y225^L (2)
Y24 (5)	S52^H (1), G56^H (3), D57^H (1)
Y42 (4)	Y164^L (4)
F44 (11)	Y223^L (4), R228^L (7)
A45 (1)	V101^H (1)

[a]criteria based on interatomic distances ≤ 4.0 Å.

[b]numbers in parentheses refer to the number of van der Waals contacts that residue forms.

TABLE S3. Accessible and Buried surface areas (ASA/BSA)[a] of residues at the scFv 9004G-Cn2 interface[b]

9004G region	9004G residue	ASA (Å^2)	BSA (Å^2)
CDR H1	N31^H	66.1	24.8
	Y32^H	68.6	17.4
	A33^H	33.8	31.6
framework H2	H35^H	30.8	18.4
	W47^H	73.0	6.4
	G50^H	5.2	5.2
CDR H2	I51^H	3.5	2.3
	S52^H	30.1	30.1
	R53^H	138.0	100.5
	S54^H	95.4	23.3
	G56^H	67.0	29.3
	D57^H	104.9	94.1
	I58^H	74.9	17.5
framework H3	D59^H	76.5	44.8
CDR H3	G99^H	7.1	4.2
	V101^H	158.1	110.7
	G102^H	78.7	29.0
CDR L1	R162^L	138.7	18.9
	Y164^L	78.4	47.2
CDR L3	Y223^L	75.0	37.3
	R224^L	74.7	21.6
	Y225^L	80.2	9.0
	S226^L	103.3	36.3
	R228^L	167.7	69.1

Cn2 region	Cn2 residue	ASA (Å^2)	BSA (Å^2)
β_1 strand	Y4	37.7	6.9
β-turn	D7	40.7	27.2
	T10	58.9	20.9
	C12	38.1	18.9
	K13	78.6	28.5
	Y14	58.9	32.0
	E15	129.3	129.3
	C16	2.4	2.4
	L17	142.7	142.7
	K18	153.4	54.5
	L19	103.4	48.5
	N22	20.0	8.0
α-helix	Y24	79.5	75.0
	R27	140.4	31.5
	E28	19.5	6.7
β_2 strand	Y42	117.9	61.2
	A43	69.2	67.0
	F44	104.7	104.7
B_3 strand	A45	9.7	7.4

[a]values according to results obtained using the PISA server.

[b]criteria used for the interacting residue assignment was a BSA change of at least 2 Å^2 upon complex formation.

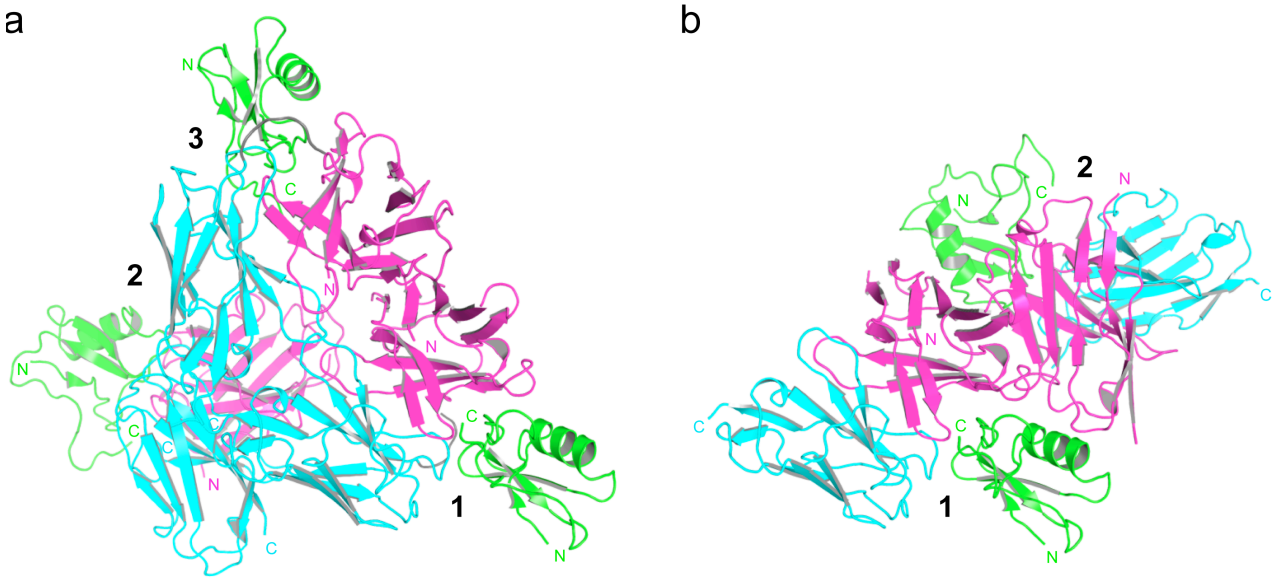

FIGURE S1. Asymmetric unit of the two structures of the complex 9004G-Cn2. ***a.*** Asymmetric unit of the structure in the space group $P2_12_12_1$. In this structure, a segment of 1-5 residues of the linker $(Gly_4–Ser)_3$ that connects V_H and V_L domains of 9004G was visible in the complexes. ***b***, Asymmetric unit of the structure in the space group $F23$. Two regions of the V_H domain of complex 1 are involved in crystal contacts both with the V_H domain and the Cn2 of complex numbered as 2. These contacts are exclusively found in this structure. Cn2 toxins are colored in green and V_H and V_L domains of 9004G are colored magenta and cyan, respectively.

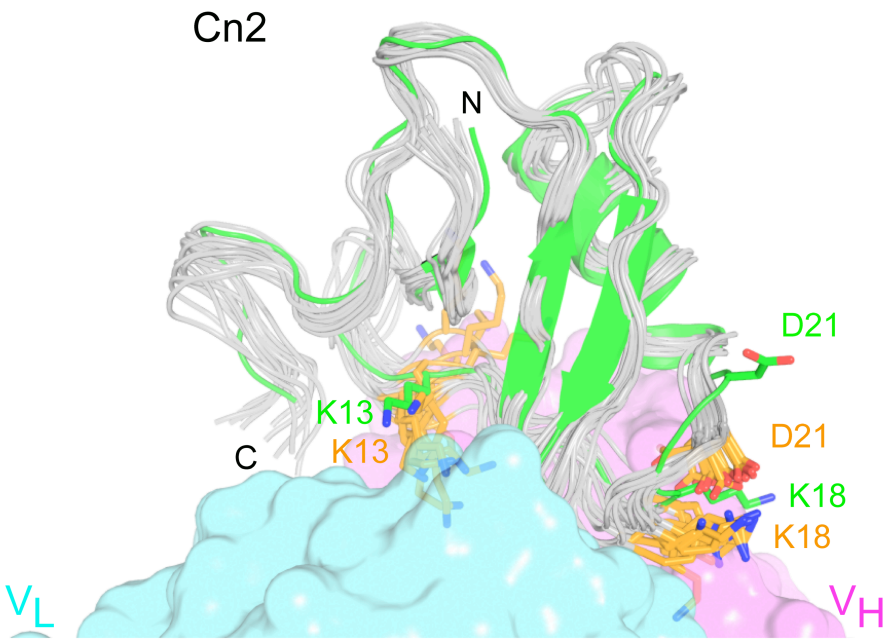

FIGURE S2. The structure of Cn2 exhibits a conformational change caused by the binding to the scFv 9004G. Superposition of the structure of Cn2-9004G complex (Cn2 is colored in green and the scFv 9004G is shown as surface presentation with the V_H and V_L domains colored in magenta and cyan, respectively) and 15 NMR structural models (colored in gray; PDB entry 1CN2) give an rmsd of 1.4 ± 0.1 Å (65 common residues). The major structural differences (rmsd ≥ 3 Å) between residues of Cn2 involved in the interface of the complex and the NMR models are in K13, K18 and D21. The segment between residues K18 and D21 (side chains colored in orange) undergoes a significant rearrangement upon binding of 9004G. This rearrangement may result from steric hindrances between residues K18 and $D59^H$ and the opposite electrostatic surface between residues D21 and $D57^H$. Residue K13 lies perpendicular with respect to its position in the NMR models (not shown). This change is due to a spatial hindrance produced by residue $V101^H$. For clarity, residues of the scFv 9004G are not shown.

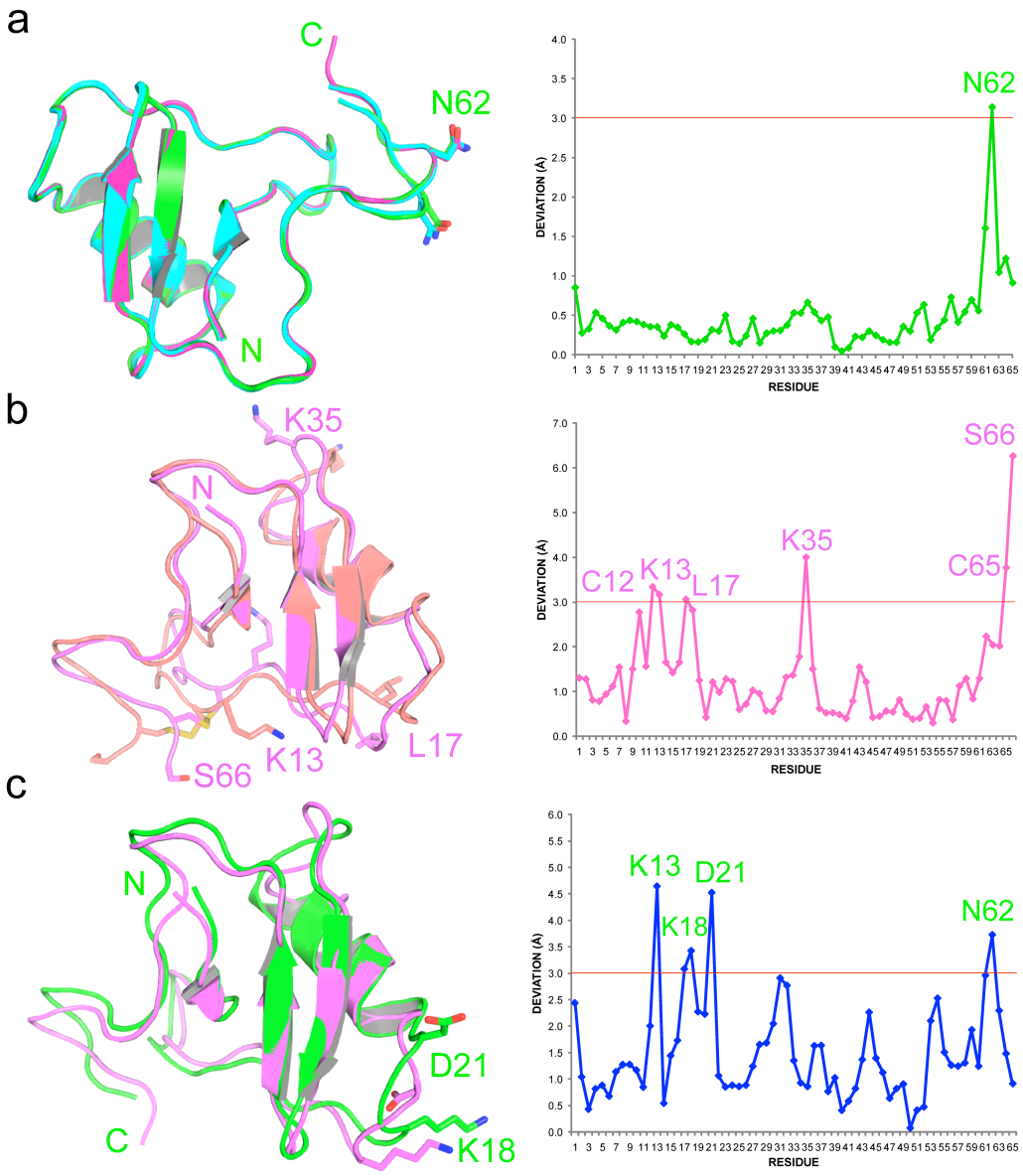

FIGURE S3. The crystal structure of Cn2 shows an alteration in the segment K18 to D21 when compared with the structure of Cn2 in solution. ***a***. Left panel, superposition of the five structures of Cn2 in asymmetric unit of the Cn2-9004G complex at 1.9 (two Cn2 molecules) and 2.5 (three Cn2 molecules) Å resolution. Right panel, rms deviations calculated between the two structures (overall rmsd 1.1 Å). Differences in residue N62 are due to the peptide bond between P61 and N62 being *cis* conformation in the 2.5 Å structure. ***b***. Left panel, superposition of two representative models of the NMR structure of Cn2 (PDB code 1CN2). Side chains of residues with the major differences (rmsd ≥ 3 Å) are shown. Right panel, rms deviations calculated between the two structures (overall rmsd 2.8 Å). Residues K13, L17, K35 and S66 are usually more flexible in the majority of the NMR models. ***c***. Left panel, superposition of the Cn2 structure in the X-ray and NMR models. Only the side chains of residues that do not vary intrinsically in the X-ray structures and the NMR models are shown (K18 and D21). Right panel, rms deviations calculated between the two structures (overall rmsd 1.8 Å). The segment between residues K18 and D21 undergoes a significant rearrangement upon binding of 9004G (Fig S2).

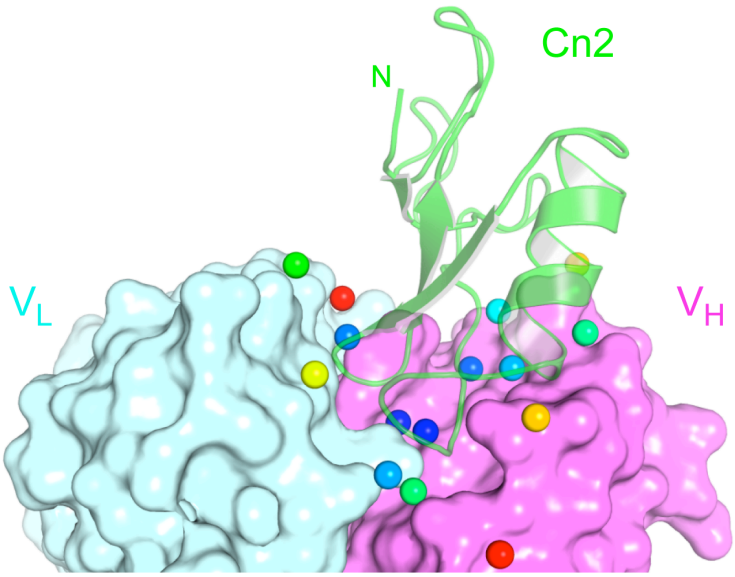

FIGURE S4. Water molecules at the interface of the complex 9004G-Cn2 partially mediate the binding of the antibody to Cn2. Water molecules that mediate hydrogen bonds at the 9004G-Cn2 interface are depicted as spheres colored according to its *B* values (RGB color scale, blue for lower B values, Table S1). Note that water molecules that are buried in a cavity at the center of the interface have a lower *B* factor than water molecules that are at the periphery of the complex (The mean *B* value for the 15 water molecules is 24 $Å^2$). These waters (colored in dark blue) play a subtle role in the stability of the complex. Cn2 is represented as cartoon and colored in green. The scFv 9004G is represented as surface with the V_H and V_L domains colored in magenta and cyan, respectively.

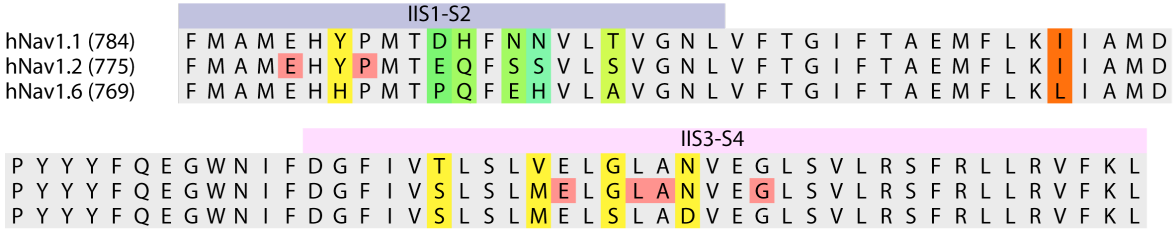

FIGURE S5. Amino acid sequence alignment of the region from IIS1-S2 to S4 segments of the domain II of human Nav1.x channels affected by Cn2, Css2 and Css4 β-scorpion toxins (1), (2)). From top to bottom the following accession numbers have been used: P35498, Q99250 and Q9UQD0. Above the sequence of hNav1.1, the IIs1-S2 (blue stripe) and the IIS3-S4 (light pink stripe) segments are marked. The amino acid changes were colored from cyan to red scale by relative conservation (red for more conserved). The red boxes in the hNav1.2 row show the positions of the amino acids altered by Cestèle *et al*. (3), (4) which was shown to decrease considerably the affinity of Css4 for its receptor site on sodium channels.

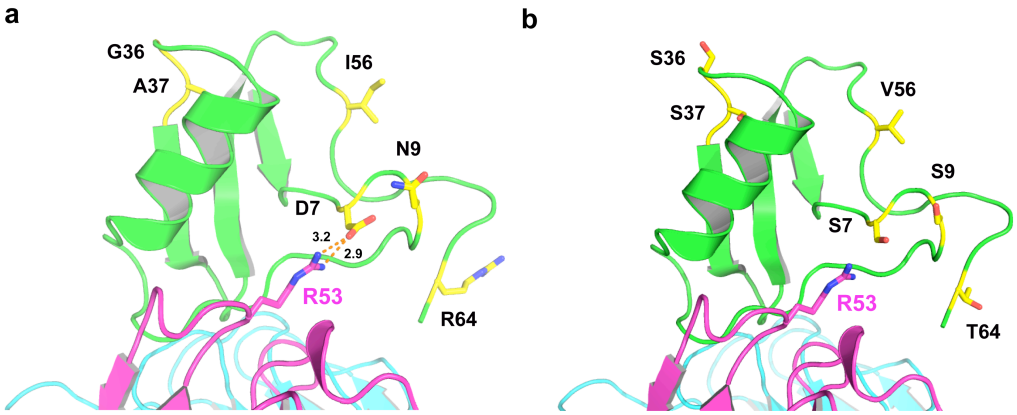

FIGURE S6. Structural basis for neutralization of two different scorpion toxins with one single-chain antibody fragment. Residues that differ between Cn2 (**a**) and Css2 toxins (model inferred from (a) and shown in (**b**)) are depicted in yellow sticks (see also Fig. 4). Among the residues that are different, only one contacts the antibody (residue 7, which in the scFv 9004G-Cn2 complex forms two salt bridges with $R53^{H}$ (see Table 2).

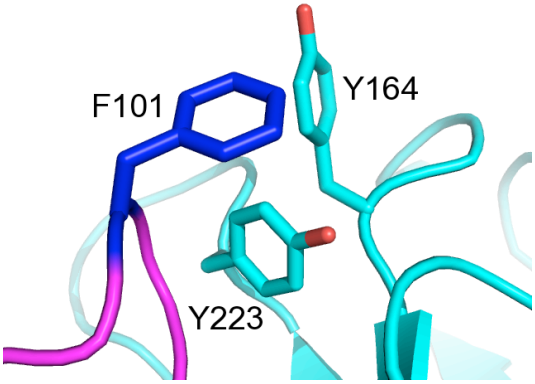

FIGURE S7. Structural environment of the V101F^{H} mutation in scFv 9004G. A model of the V101F mutation in scFv 9004G is presented. Mutation V101F^{H} promotes the formation of a small, hydrophobic cluster on the surface of the antibody along with residues Y164^{L} and Y223^{L}. This single mutation yields scFv LR (5), a more stable antibody than scFv9004G.

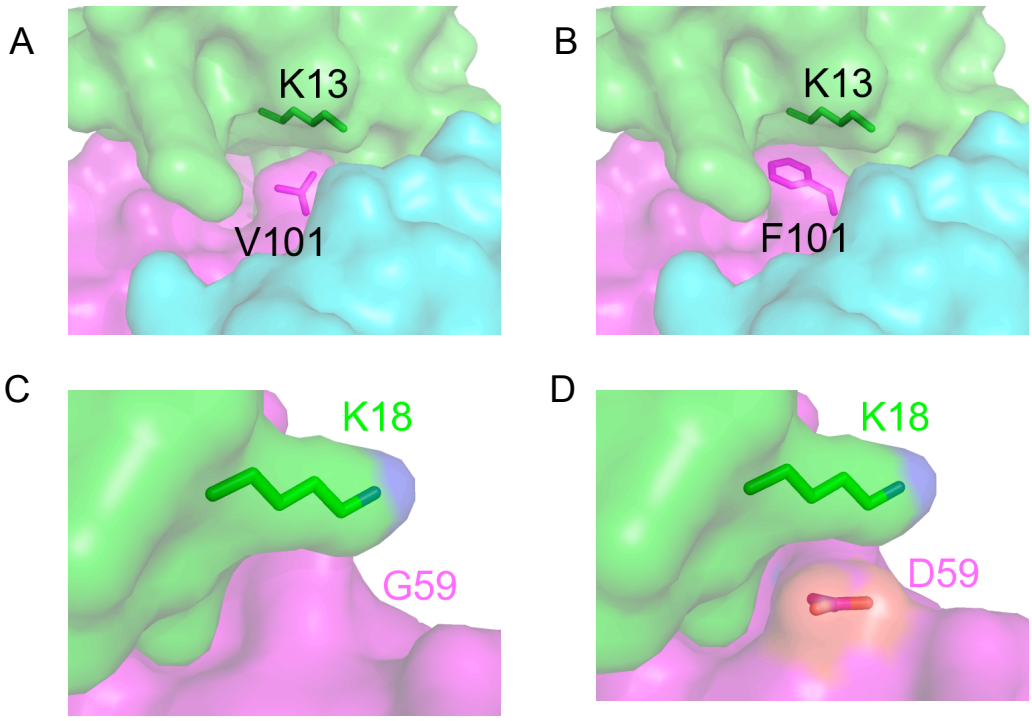

FIGURE S8. The structural environment of key scFvs mutants increases toxin recognition. A and B. Mutation V101F^{H} (see Figure S7) could promote the formation of a more extensive interface, in particular through stacking with residue K13 of the toxin. **C and D.** Mutation G59D^{H} increases recognition to Css2 in a significant manner (5). This change is present in scFv 9004G and increases interaction surface area with the toxin while providing electrostatic interactions with K18.

REFERENCES

1. Schiavon, E., Sacco, T., Cassulini, R. R., Gurrola, G., Tempia, F., Possani, L. D., and Wanke, E. (2006) *J Biol Chem* **281**, 20326-20337
2. Estrada, G., Garcia, B. I., Schiavon, E., Ortiz, E., Cestele, S., Wanke, E., Possani, L. D., and Corzo, G. (2007) *Biochim Biophys Acta* **1770**, 1161-1168
3. Cestele, S., Yarov-Yarovoy, V., Qu, Y., Sampieri, F., Scheuer, T., and Catterall, W. A. (2006) *J Biol Chem* **281**, 21332-21344
4. Cestele, S., Qu, Y., Rogers, J. C., Rochat, H., Scheuer, T., and Catterall, W. A. (1998) *Neuron* **21**, 919-931
5. Riano-Umbarila, L., Contreras-Ferrat, G., Olamendi-Portugal, T., Morelos-Juarez, C., Corzo, G., Possani, L. D., and Becerril, B. (2011) *J Biol Chem* **286**, 6143-6151